

# Optimal eVTOL Fleet Dispatch for Urban Air Mobility and Power Grid Services

Syed A.M. Shihab\* and Peng Wei†  
Iowa State University, Ames, IA, USA 50011

Jie Shi‡ and Nanpeng Yu§  
University of California, Riverside, CA, USA 92521

Fuel cost has always been the highest contributor to operating cost for airlines. In the context of Urban Air Mobility (UAM), for a company providing aerial ridesharing services, the cost of electric energy it consumes from the power grid will be the dominating cost factor. Unlike fuel, the electricity market is highly dynamic in terms of pricing and incentives. It often provides considerable amount of monetary compensation for consumers to help balance generation and load in the power system. In this work, we develop an optimal fleet dispatch framework for electric vertical take-off and landing (eVTOL) aircraft to transport passengers and provide power grid services either separately or together. In addition to vehicle dispatching, the framework can also optimally price passenger trips taking place at different routes at different times. The eVTOL vehicle fleet operations was subjected to two sources of uncertainties, which are the pricing/incentive stochasticity from the dynamic electricity market, and the passenger demand uncertainty due to the stochastic trip requests. We investigate the trade-off among multiple revenue and cost sources for eVTOL fleet operations. The major objectives of this work include: (1) maximizing the first revenue source generated from transporting passengers; (2) maximizing the second revenue source generated from providing frequency regulation services to the power grid; and (3) reducing the operating and charging costs. The major benefits of this work include: (1) maximizing the revenue from eVTOL fleet operation, which will result in a more profitable aerial ride sharing company; (2) lowering the riding cost for passengers, which will make the aerial ride sharing more affordable to customers; and (3) enhancing the reliability and stability of modern smart grid. The results demonstrate that UAM carriers can earn more profit by dispatching the eVTOL fleet to provide both UAM travel and power grid services simultaneously than providing only one of the services.

## I. Nomenclature

$N$	=	set of nodes or vertiports in the UAM network
$A$	=	set of arcs in the UAM network
$G$	=	a UAM network composed of $N$ and $A$
$T$	=	set of predefined time steps in the operational period
$K$	=	set of all eVTOL vehicles
$N'$	=	set of all space-time (ST) nodes, where each ST node = (node,time)
$A'$	=	set of all ST arcs
$G'$	=	a ST UAM network composed of $N'$ and $A'$
$\hat{i}, \hat{j}, \hat{h}$	=	indices to denote nodes in $N$
$(\hat{i}, \hat{j})$	=	arc in $A$
$r, s$	=	indices to denote time steps
$h, i, j$	=	indices to denote ST nodes in $N'$
$(i, j)$	=	arc in $A'$

---

\*Graduate Research Assistant, Department of Aerospace Engineering, shihab@iastate.edu. Student Member AIAA.

†Assistant Professor, Department of Aerospace Engineering, pwei@iastate.edu. Senior Member AIAA.

‡Graduate Research Assistant, Department of Electrical and Computer Engineering, jshi005@ucr.edu.

§Associate Professor, Department of Electrical and Computer Engineering, nyu@ece.ucr.edu.

$k$	=	index to denote an eVTOL in $K$
$q_{ij}$	=	total potential demand in ST arc $(i, j)$
$e_{ij}$	=	energy required to fly an eVTOL in ST arc $(i, j)$
$E_{max}^k$	=	battery capacity of eVTOL $k$
$c_{ij}$	=	cost of operating a flight in ST arc $(i, j)$
$\beta$	=	slope of demand curve
$C$	=	passenger capacity of eVTOLs
$u_{\hat{i}}$	=	eVTOL capacity of vertiport $\hat{i}$
$z$	=	total operating profit
$E_i^k$	=	energy of eVTOL $k$ at ST node $i$
$p_{ij}$	=	fare charged to passengers traveling in ST arc $(i, j)$
$x_{ij}^k$	=	binary variable indicating whether eVTOL $k$ is dispatched in ST arc $(i, j)$
$x_i^k$	=	binary variable indicating whether eVTOL $k$ is stationed at starting ST node $i$ , where $i = (\hat{i}, 0)$
$d_{ij}$	=	expected passenger demand in ST arc $(i, j)$ for a fare of $p_{ij}$
$C_{ij}$	=	number of seats available for transporting passengers in ST arc $(i, j)$
$E_{ij}^k$	=	energy expenditure of eVTOL $k$ in ST arc $(i, j)$
$w_{ij}$	=	number of passengers transported in ST arc $(i, j)$
$LMP_r$	=	locational marginal price of electricity given by the electricity market at time step $r$
$B_r^U$	=	revenue from committing 1MWh of battery capacity to regulation up service
$B_r^D$	=	revenue from committing 1MWh of battery capacity to regulation down service
$p_r^U$	=	the ratio between real regulation up signal and the provided capacity at time step $r$
$p_r^D$	=	the ratio between real regulation down signal and the provided capacity at time step $r$
$r_{ij}^{U,k}$	=	provided capacity of regulation up service for eVTOL $k$ in ST arc $(i, j)$
$r_{ij}^{D,k}$	=	provided capacity of regulation down service for eVTOL $k$ in ST arc $(i, j)$
$g_{ij}^k$	=	charging rate of eVTOL $k$ in ST arc $(i, j)$
$T^l$	=	time interval of each time step
$\gamma$	=	battery's self-discharge rate
$P_{max}$	=	maximum power transferred between an eVTOL and the power grid

## II. Introduction

### A. Urban Air Mobility with eVTOLs

Getting from point A to point B in busy metropolitan areas is often an unpleasant travel experience for us as it involves moving through dense traffic and frequent lights, causing us to burn a wasteful amount of our gas, time, and energy. Fortunately, this travel experience is expected to dramatically improve soon for commuters, with respect to cost, time, and comfort, with the advent of UAM: a promising new mode of transportation conceptualized to leverage unused airspace with fully electric helicopter-like aircraft called eVTOLs. Throughout the rest of the paper, the terms “eVTOL” and “vehicle” are used interchangeably. As there are helipads for helicopters, there will be *vertiports* for eVTOLs, which will be located strategically within the cities to provide designated spaces for the take off, landing and charging of the eVTOLs. Additionally, in this work, we envision that a eVTOL parked at a vertiport can be used for providing frequency regulation (balancing the power grid) services to the power grid through charging (buying electricity from the market) and discharging (selling electricity to the market).

UAM is envisioned to support a broad range of operations, such as passenger transport and cargo delivery. With many organizations, such as NASA, Uber, Airbus, Volocopter, Aurora Flight Sciences, Joby Aviation, and Kitty Hawk, actively overcoming market feasibility barriers, aviation technology gaps, and operational challenges associated with the implementation and operation of UAM [1–10], these eVTOLs, designed to ferry passengers and goods on aerial virtual highways, are projected to hit the road — or, in this case, the air — soon. Several cities have been identified to feature a feasible infrastructure and an economically viable market for UAM, such as Dubai in United Arab Emirates, Sao Paulo in Brazil, and San Francisco, Los Angeles, and Dallas-Fort Worth metroplex in USA. These cities have drawn the interest of government, academia and industry towards implementing UAM in the near future [1, 11–13].

## **B. Electricity Markets**

In the United States, electricity can be traded in wholesale and retail markets [14, 15], which operate similarly to wholesale and retail markets for other products [16]. The current wholesale electricity trading process operates as a “multi-settlement” system that consists of two stages: the day-ahead energy market and real-time energy market [17]. The day ahead electricity market allows participants to trade electricity one day before the operating day. The vast majority of system generation and load are committed at this stage based on optimal operating condition, producing relatively stable market clearing prices. The real-time market lets market participants sell and buy electricity for each individual hour in the operating day. It balances the differences between the day-ahead commitments and actual real-time demands. The clearing prices of this stage can be volatile depending on the actual power system operating condition. It is worth noting the electricity price in the wholesale electricity market is formally called locational marginal price (LMP) due to its variability with respect to location. The factors which determine the day-ahead and real-time LMPs are the supply offers from generators, demand bids from load serving entities, and the system operating conditions. The LMPs have three key components, the energy component, the congestion component, and the network loss component [18].

In addition to the above two energy markets, there are a few types of ancillary service products, which are essential in maintaining reliable operations and stability of the power systems [19]. The two most important ancillary services are the frequency regulation and reserves. The design objective of frequency regulation service is to bridge the small gaps between scheduled load and generation and actual load and generation. The reserves, on the other hand, are used to compensate for the large unexpected generation deficiencies in case of contingencies. Most of the US electricity markets have two types of reserves: spinning reserve and non-spinning reserve. We refer interested readers to [20] for more information and details about electricity markets.

## **C. Battery Degradation**

The degradation of battery depends on the depth of discharge, the current rate, and the mean state-of-charge (SoC) of the cycles. Therefore, different dispatch and schedule of eVTOLs can result in different degradation rates and hence lifetime of their batteries. Given that batteries account for a significant part of the bill, the process of battery degradation needs to be addressed in our eVTOL fleet dispatch model. There are several existing approaches that incorporate the battery degradation process into the optimization framework. See [21] and [22] for examples.

## **D. Providing Frequency Regulation Services with eVTOLs**

A large fleet of eVTOLs as a single entity is more than a transportation tool. It has great potential in providing frequency regulation services to the power grid based on the following facts. First, the overall battery capacity and power of a large eVTOL fleet can meet the requirements of frequency regulation market [23]. Second, batteries of eVTOLs can easily follow the dynamic frequency regulation signals given by the power system controller. Moreover, the time ranges of transportation demand peaks are usually different from that of the electricity consumption peaks, making eVTOL fleet naturally advantageous in demand response. The immediate benefits of providing frequency regulation services with eVTOLs are:

- Increasing the revenue from eVTOL fleet operation with additional revenue sources, which will result in a more profitable aerial ride sharing company;
- Reducing the riding cost for passengers by carefully managing the battery degradation cost among other operation costs, which will make the aerial ride sharing more affordable to customers;
- Enhancing the reliability and stability of modern smart grid.

The rest of the paper is organized as follows. In Section III, the problem of eVTOL dispatching for UAM operations is formally defined. The modeling approach used for formulating the eVTOL dispatch problem is then discussed in Section IV. The formulation of three types of models for providing the passenger transportation and frequency regulation services separately and together are then presented in Section V. The simulator used and the results generated are next discussed in Sections VI and VII respectively. Finally, a summary of the findings of this work is given in VIII.

## **III. Problem Statement**

UAM services have been largely envisioned to be an on-demand aerial ridesharing travel service, but it may also be operated based on a fixed predetermined timetable similar to how airlines operate scheduled flights. In [24], we conceptualized a new form of UAM service, the hybrid UAM service, in an attempt to combine the best features of on-demand and scheduled travel services. For each of these services, we have also developed operations management

(OM) models — namely, the scheduler, dispatcher, and hybrid scheduler-dispatcher respectively — based on operational constraints and demand forecasts to determine scheduling and dispatching decisions that would maximize profit in the operational period. The scheduler can be used to determine the optimal flight timetable that would capture the daily, weekly or monthly periodic and stable passenger demand, and the dispatcher can be used to optimally assign vehicles to passengers in real-time to satisfy the ad-hoc or on-demand passenger trip requests. The only source of revenue considered was the fares paid by the booked passengers. The potential additional revenue from providing frequency regulation services and the time-varying charging costs as determined by the dynamic electricity market conditions were not considered.

In this paper, we extend the dispatching OM model of our previous work [24] by considering: (1) a more realistic charging process under varying electricity price given by the electricity market; (2) a more realistic battery model that includes degradation process in the optimization framework; (3) the option of providing frequency regulation service to the power grid by charging and discharging eVTOL batteries to gain additional revenues. This implies a more complex objective function along with additional decision variables and energy constraints in the OM model to enable the UAM carrier to make a profit-maximizing trade-off on how and when to use its vehicles for providing travel and energy-related services based on real-time demand and power grid conditions. As the decision maker in the problem is considered to be a commercial UAM carrier, the objective function is considered to be maximization of profit to reflect the decision maker’s true preference. In the case of a government-owned UAM carrier, the true preference may not necessarily be profit. Instead, it might be maximization of reliability of service or frequency of flights, or minimization of cost or fare, etc. For more details on preference modeling for government-owned systems, interested readers are referred to [25].

#### IV. Modeling Approach

The architecture of the eVTOL fleet dispatching optimization framework, depicted in Fig. 1, shows the inputs and outputs of the OM model. Real time trip requests, passenger mobility data, geography, wealth and demographics data can be used to forecast the time-varying demand of the origin-destination (O-D) markets or routes in the network. The demand forecast combined with other problem parameters, namely, the planning horizon, eVTOL fleet characteristics, network configuration, and electricity market prices, are then used to formulate the OM model. The planning horizon specifies the length of the planning period or the look-ahead time span. The optimal dispatching solution for the planning horizon specified can then be found by solving the problem using a suitable optimization algorithm. To be able to effectively serve real-time demand and react to changes in market conditions, the model would need to be solved repeatedly after every certain interval of time as specified by the planning frequency in real-time with updated problem parameters. Based on the vehicle dispatching carried out by the OM model during the period of operation, the battery conditions of the vehicles would need to be updated after every certain interval of time to take into account battery degradation effects.

An example of an UAM network is depicted in Fig. 2a. It consists of 3 vertiports, completely connected with each other through 6 distinct routes or O-D markets. The nodes represent the vertiports and the arcs the distinct O-D markets. So, if we let  $G$  represent a UAM network, then  $G = (N, A)$ , where  $N$  is the set of all nodes and  $A$  the set of all arcs. In practice, this type of UAM network may be set up in any large metropolitan area, such as Dallas-Fort Worth (DFW) metroplex and Los Angeles, and different facilities such as municipal airports, helipads, and roofs of building, may be used as vertiports. All vertiports are assumed to have a certain number of high voltage charging/discharging stations, maintenance facilities, parking spaces and takeoff and landing areas. Although, the routes are illustrated by straight lines, they may in practice take any shape, such as piecewise linear or curve, comprising of a number of intermediate waypoints. Given the average flight distances, travel times, and required energy for flight in each route, the computation of optimal dispatch solutions is independent of the exact flight path.

Expanding each node across time results in the space-time (ST) UAM network illustrated in Fig. 2b. The nodes (white circles) along the horizontal lines are referred to as ST nodes and the arcs (colored arrows) going from one ST node to another as ST arcs. Each ST node  $i$  has two components: node and time. So,  $i = (\hat{i}, r)$ , where  $\hat{i}$  denotes the node and  $r$  the time instance. A ST arc connecting ST node  $i$  and ST node  $j$  is represented as  $(i, j)$ . So, if we let  $G'$  represent a ST UAM network, then  $G' = (N', A')$ , where  $N'$  is the set of all ST nodes and  $A'$  the set of all ST arcs. The time axis or operational time has been sliced into fixed intervals of time called time steps. The duration of each time step ( $T^I$ ) is considered to be 30 minutes long based on the assumption that trips in each route can be completed within 30 minutes. The total time for each trip includes the passenger boarding time, flight time, and eVTOL turnaround time. The set of all time steps is denoted by  $T$ . An extension of schedule maps previously used by airlines, the ST network provides a visual representation of the movement of eVTOLs across vertiports and time via two types of arcs: ground arc (solid arrow)

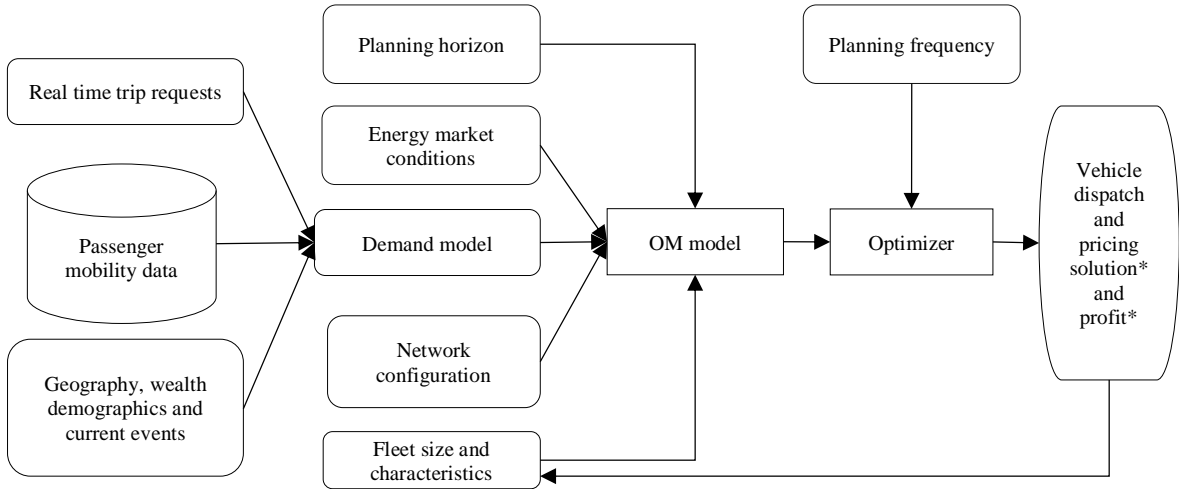
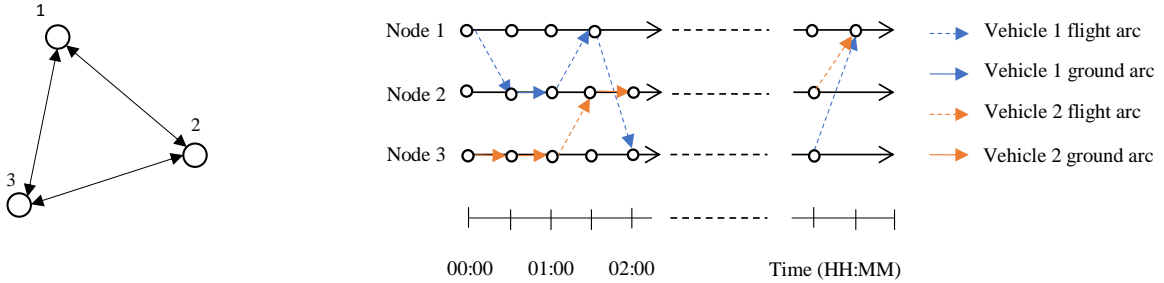


**Fig. 1 Architecture of the eVTOL fleet dispatching framework**



**(a) A time stationary three vertiport network**

**(b) A space-time network showing flight and ground arcs**

**Fig. 2 An UAM network**

and flight arc (dashed arrow). Fig. 2b shows the paths of two vehicles (orange and blue) along the ST network. Vehicles on ground arcs (horizontal arcs) are either idle, charging, or providing frequency regulation services whereas vehicles on flight arcs (non-horizontal) are either transporting passengers or getting repositioned from one vertiport to another. Departure and arrival times of each flight arc are the times associated with the arc's origin ST node and destination ST node respectively. The time duration of each ST flight and ground arc is considered to be equal to  $T^l$ . A ST arc  $(i, j)$  is a ground arc if the origin ST node and destination ST node have the same corresponding vertiport. Mathematically, this is represented as  $i = (\hat{i}, r)$  and  $j = (\hat{i}, s)$ . Conversely, a ST arc  $(i, j)$  is a flight arc if the origin ST node and destination ST node have different corresponding vertiports. Mathematically, this is represented as  $i = (\hat{i}, r)$ ,  $j = (\hat{j}, s)$  and  $\hat{i} \neq \hat{j}$ .

## V. Problem Formulation

In this section, we first introduce our base dispatch model for providing only UAM travel services, and then extend it to incorporate the energy aspects related to providing the additional service of frequency regulation. In total, we have formulated three OM models: model-TS, model-TRS and model-RS. Model-TS is intended to be used for only providing UAM travel service, model-TRS for providing both UAM travel service and frequency regulation service, and model-RS for providing only frequency regulation service.

### A. Model-TS: Base eVTOL Fleet Dispatch Model for Providing Only UAM Travel Service

Given an UAM network, fleet size and characteristics, and planning horizon, the objective of the base eVTOL dispatching problem is to assign the eVTOLs in the fleet to ST arcs within the planning horizon and determine the fares to charge in each ST arc such that the operating profit is maximized. The set of decision variables in the problem are represented by  $p_{ij}$ ,  $w_{ij}$ ,  $x_{ij}^k$ ,  $x_i^k$ ,  $E_i^k$ , and  $g_{ij}^k$ , where  $p_{ij}$  denotes the fare charged in ST arc  $(i, j)$ ,  $w_{ij}$  denotes the number of passengers transported in ST arc  $(i, j)$ ,  $x_{ij}^k$  indicates whether eVTOL  $k$  is dispatched in ST arc  $(i, j)$  or not,  $x_i^k$  indicates whether eVTOL  $k$  is stationed at starting ST node  $i = (\hat{i}, 0)$  or not,  $E_i^k$  denotes the energy of an eVTOL  $k$  at ST node  $i$ , and  $g_{ij}^k$  denotes the charging rate of eVTOL  $k$  in ST arc  $(i, j)$ . The decision variables  $p_{ij}$ ,  $E_i^k$  and  $g_{ij}^k$  are continuous,  $w_{ij}$  is integral, and  $x_{ij}^k$  and  $x_i^k$  are binary.

The objective function to be maximized is given in Eq. (1), which computes the total operating profit ( $z$ ) by subtracting the total flight operating cost ( $C_O$ ) and total charging cost ( $C_C$ ) from the total generated revenue from providing travel service ( $R_T$ ).  $R_T$ ,  $C_O$  and  $C_C$  can be computed using Eqs. (2), (3) and (4) respectively. For each ST flight arc  $(i, j)$ , the revenue generated is the total fare collected from the passengers transported in the arc ( $p_{ij}w_{ij}$ ). For each ST flight arc  $(i, j)$  and eVTOL  $k$ , the operating cost incurred is  $c_{ij}$  if eVTOL  $k$  is dispatched in arc  $(i, j)$ . For each ST ground arc  $(i, j)$  and eVTOL  $k$ , the charging cost incurred is  $g_{ij}^k LMP_r T^I$  if eVTOL  $k$  is dispatched in arc  $(i, j)$ .

$$\max z = R_T - C_O - C_C \quad (1)$$

$$R_T = \sum_{(i,j) \in A': i=(\hat{i},r), j=(\hat{j},s), \hat{i} \neq \hat{j}} p_{ij} w_{ij} \quad (2)$$

$$C_O = \sum_{k \in K} \sum_{(i,j) \in A': i=(\hat{i},r), j=(\hat{j},s), \hat{i} \neq \hat{j}} c_{ij} x_{ij}^k \quad (3)$$

$$C_C = \sum_{k \in K} \sum_{(i,j) \in A': i=(\hat{i},r), j=(\hat{i},s)} g_{ij}^k x_{ij}^k LMP_r T^I \quad (4)$$

Demand in any given ST arc  $(i, j)$  ( $d_{ij}$ ) varies with the fare charged in that arc ( $p_{ij}$ ), as shown in Eq. (5), where  $q_{ij}$  represents the total potential demand in the ST arc  $(i, j)$  and  $\beta$  is the demand slope (a measure of the passenger price sensitivity). The number of passenger seats available in any given ST arc  $(i, j)$  ( $C_{ij}$ ) is determined by the product of the seat capacity of eVTOLs ( $C$ ) and the number of eVTOLs dispatched on the given arc ( $\sum_{k \in K} x_{ij}^k$ ), as shown in Eq. (6).

$$d_{ij} = q_{ij} - \beta p_{ij}, \quad \forall (i, j) \in A' \quad (5)$$

$$C_{ij} = C \sum_{k \in K} x_{ij}^k, \quad \forall (i, j) \in A' \quad (6)$$

Clearly, the number of transported passengers in any ST arc  $(i, j)$  cannot be higher than the corresponding  $C_{ij}$  and  $d_{ij}$ . This is enforced by the constraints given in Eqs. (7) and (8). Although taking the minimum of  $C_{ij}$  and  $d_{ij}$  gives the optimal  $w_{ij}$ , this computation is not carried out directly as it would introduce a nonlinear term in the objective function.

$$w_{ij} \leq d_{ij}, \quad \forall (i, j) \in A' \quad (7)$$

$$w_{ij} \leq C_{ij}, \quad \forall (i, j) \in A' \quad (8)$$

At the start of the operational period, all vehicles must be assigned to one and only one vertiport. This vertiport assignment constraint is enforced by Eq. (9).

$$\sum_{i \in N': i=(\hat{i},0)} x_i^k = 1, \quad \forall k \in K \quad (9)$$

For any ST node  $h$  preceding the last time instance in the planning horizon, if there is a vehicle  $k$  entering it through one of its incoming arcs ( $\sum_{i \in N': (i,h) \in A'} x_{ih}^k$ ), then the same vehicle must also be leaving it through one of its outgoing arcs ( $\sum_{j \in N': (h,j) \in A'} x_{hj}^k$ ). Equations (10) and (11) enforces this vehicle flow conservation at all ST nodes at the starting

time as well as at all other times preceding the last time instance in the planning horizon respectively. The total number of time steps in the planning horizon is represented by  $|T|$ .

$$x_i^k = \sum_{j \in N': (i,j) \in A'} x_{ij}^k, \quad \forall i \in N' : i = (\hat{i}, 0), \forall k \in K \quad (10)$$

$$\sum_{i \in N': (i,h) \in A'} x_{ih}^k = \sum_{j \in N': (h,j) \in A'} x_{hj}^k, \quad \forall h \in N' : h = (\hat{h}, r), 1 \leq r \leq |T| - 1, \forall k \in K \quad (11)$$

The vertiport capacity constraints, expressed in Eqs. (12) and (13), ensure that the number of vehicles at a vertiport  $\hat{i}$  at the starting time ( $\sum_{k \in K} x_i^k$ ) as well as at all other times ( $\sum_{h \in N': (h,i) \in A'} \sum_{k \in K} x_{hi}^k$ ) in the planning horizon does not exceed the vertiport's capacity ( $u_{\hat{i}}$ ).

$$\sum_{k \in K} x_i^k \leq u_{\hat{i}}, \quad \forall i \in N' : i = (\hat{i}, 0) \quad (12)$$

$$\sum_{h \in N': (h,i) \in A'} \sum_{k \in K} x_{hi}^k \leq u_{\hat{i}}, \quad \forall i \in N' : i = (\hat{i}, r), r \geq 1 \quad (13)$$

The energy constraints are expressed in the following equations. The energy of an eVTOL  $k$  at ST node  $i$  ( $E_i^k$ ) can take any value between 0 (state of zero charge) and the battery capacity (state of full charge) of eVTOL  $k$  ( $E_{max}^k$ ). This constraint is stated in Eq. (14). At the first time instant, vehicles are assumed to have full energy. This is defined by Eq. (15), which specifies that, at the starting time, the energy of a vehicle  $k$  at ST node  $i$  ( $E_i^k$ ), where  $i = (\hat{i}, 0)$ , is equal to its full battery capacity ( $E_{max}^k$ ) if the vehicle is present at that node, and, otherwise, it is zero. When an eVTOL  $k$  is dispatched in a ST arc  $(i, j)$ , its energy at the destination node  $j$  ( $E_j^k$ ) is computed using Eq. 16, where  $\gamma$  is the battery's self discharge rate,  $\gamma E_i^k$  is the battery's self discharge amount, and  $E_{ij}^k$  is the energy expenditure of eVTOL  $k$  in ST arc  $(i, j)$ . The resistive loss component of batteries has been assumed to be negligible in this equation. Eqs. (17) and (18) specify the value of  $E_{ij}^k$  in ST flight and ground arcs respectively. For a ST flight arc  $(i, j)$ , it is considered to be equal to a positive constant  $e_{ij}$ . For a ST ground arc  $(i, j)$ ,  $E_{ij}^k$  will be zero if the eVTOL  $k$  is idle and negative if it is charging (or gaining energy). The total charging amount is equal to  $g_{ij}^k T^I$ , where  $g_{ij}^k$  is the charging rate of eVTOL  $k$  in ST arc  $(i, j)$  and  $T^I$  is the duration of a time step. The value of  $g_{ij}^k$  is constrained to be positive and bounded within 0 and  $P_{max}$ , the maximum power transferred between an eVTOL and the power grid, as shown in Eq. 19. When the eVTOL  $k$  is used to provide frequency regulation service, the value of  $g_{ij}^k$  is allowed to take negative values so that the battery of eVTOL  $k$  can discharge to the power grid, as discussed in Section V.B. Lastly, Eq. 20 ensures that the charging amount of eVTOL  $k$  in ST ground arc  $(i, j)$  ( $g_{ij}^k T^I$ ) does not exceed the charge deficiency of eVTOL  $k$  at origin ST node  $i$  ( $E_{max}^k - E_i^k$ ).

$$0 \leq E_i^k \leq E_{max}^k, \quad \forall i \in N', \forall k \in K \quad (14)$$

$$E_i^k = x_i^k E_{max}^k, \quad \forall i \in N' : i = (\hat{i}, 0), \forall k \in K \quad (15)$$

$$E_j^k = ((1 - \gamma)E_i^k - E_{ij}^k) \cdot x_{ij}^k, \quad \forall j \in N' : j = (\hat{j}, s), s > 0, i = (\hat{i}, r), s = r + 1, (i, j) \in A', \forall k \in K \quad (16)$$

$$E_{ij}^k = e_{ij}, \quad \forall (i, j) \in A' : i = (\hat{i}, r), j = (\hat{j}, s), \hat{i} \neq \hat{j}, \forall k \in K \quad (17)$$

$$E_{ij}^k = -g_{ij}^k T^I, \quad \forall (i, j) \in A' : i = (\hat{i}, r), j = (\hat{j}, s), \hat{i} = \hat{j}, \forall k \in K \quad (18)$$

$$0 \leq g_{ij}^k \leq P_{max}, \quad \forall (i, j) \in A' : i = (\hat{i}, r), j = (\hat{j}, s), \hat{i} = \hat{j}, \forall k \in K \quad (19)$$

$$g_{ij}^k \cdot T^I \leq E_{max}^k - E_i^k, \quad \forall (i, j) \in A' : i = (\hat{i}, r), j = (\hat{j}, s), \hat{i} = \hat{j}, \forall k \in K \quad (20)$$

The base OM optimization model formulated above has a quadratic objective function. All other equations are linear except the constraint given in Eq. 16. The order of nonlinearity of Eq. 16 depends on the the time  $s$  corresponding to

the ST node  $j$ , where  $j = (\hat{j}, s)$ . When  $s = 1$ , the equation is a second order polynomial. For each unit increment of  $s$ , the order of the equation also increases by one. To deal with this increasing nonlinearity, the variable  $E_j^k$  is treated as a decision variable which causes the equation to become a quadratic polynomial for all ST node  $j$  and eVTOL  $k$ . Given the type of equations and decision variables described above, the base dispatch optimization problem is a non-convex mixed integer quadratically constrained quadratic program (MIQCQP).

## B. Model-TRS: eVTOL Fleet Dispatch Model for Providing Both UAM Travel and Frequency Regulation Services

In this subsection, we will extend model-TS, the base dispatch model, to add the capability of providing regulation services to the power grid to it by considering additional energy terms and equations associated with such service. The new objective is now composed of four components as shown in Eq. (21).

$$\max z = R_T + R_R - C_O - C_C \quad (21)$$

In this equation, the terms  $R_T$ ,  $C_O$  and  $C_C$  are the same as before. The additional term  $R_R$  represents the revenue generated from providing regulation services and it is defined in the following equation.

$$R_R = \sum_{k \in K} \sum_{(i,j) \in A' : i=(\hat{i},r), j=(\hat{j},s)} \mathbf{1}^T \begin{bmatrix} LMP_r \cdot p_r^U & -LMP_r \cdot p_r^D \\ B_r^U & B_r^D \end{bmatrix} \begin{bmatrix} r_{ij}^{U,k} \\ r_{ij}^{D,k} \end{bmatrix} x_{ij}^k T^I \quad (22)$$

$B_r^U$  and  $B_r^D$  are revenues from committing 1MWh of battery capacity to regulation up and down services respectively.  $r_{ij}^{U,k}$  and  $r_{ij}^{D,k}$  are two new sets of decision variables. They denote the provided capacities of regulation up and down services for the  $k$ th eVTOL at ST arc  $(i, j)$  respectively.  $p_r^U$  and  $p_r^D$  define the ratios between real regulation up and down signals and the provided capacities respectively. Note that  $g_{ij}^k$  can be negative now, indicating that the corresponding eVTOL is selling electricity back to the power grid.

We keep most of the original constraints the same but replace the energy constraints Eqs. (18)-(20) with the following set of equations:

$$E_{ij}^k = (-g_{ij}^k + p_r^U r_{ij}^{U,k} - p_r^D r_{ij}^{D,k}) \cdot T^I, \quad \forall (i, j) \in A' : i = (\hat{i}, r), j = (\hat{j}, s), \hat{i} = \hat{j}, \forall k \in K \quad (23)$$

$$-P_{max} \leq -g_{ij}^k + p_r^U r_{ij}^{U,k} - p_r^D r_{ij}^{D,k} \leq P_{max}, \quad \forall (i, j) \in A' : i = (\hat{i}, r), j = (\hat{j}, s), \hat{i} = \hat{j}, \forall k \in K \quad (24)$$

$$-g_{ij}^k + r_{ij}^{U,k} \leq P_{max}, \quad \forall (i, j) \in A' : i = (\hat{i}, r), j = (\hat{j}, s), \hat{i} = \hat{j}, \forall k \in K \quad (25)$$

$$g_{ij}^k + r_{ij}^{D,k} \leq P_{max}, \quad \forall (i, j) \in A' : i = (\hat{i}, r), j = (\hat{j}, s), \hat{i} = \hat{j}, \forall k \in K \quad (26)$$

$$(-g_{ij}^k + r_{ij}^{U,k}) \cdot T^I \leq E_i^k, \quad \forall (i, j) \in A' : i = (\hat{i}, r), j = (\hat{j}, s), \hat{i} = \hat{j}, \forall k \in K \quad (27)$$

$$(g_{ij}^k + r_{ij}^{D,k}) \cdot T^I \leq E_{max}^k - E_i^k, \quad \forall (i, j) \in A' : i = (\hat{i}, r), j = (\hat{j}, s), \hat{i} = \hat{j}, \forall k \in K \quad (28)$$

$$r_{ij}^{U,k}, r_{ij}^{D,k} \geq 0, \quad \forall (i, j) \in A' : i = (\hat{i}, r), j = (\hat{j}, s), \hat{i} = \hat{j}, \forall k \in K \quad (29)$$

Eq. (24)-(26) constrain the power transfer rate between an eVTOL and the power grid to be within the maximum limit. Eq. (27)-(28) ensure that the battery capacity is not exceeded. Eq. (29) ensures that the provided capacities of regulation up and down are greater than or equal to zero.

Note that  $E_{max}^k$  will change due to the battery degradation. This value would have to be updated in regular intervals as defined by the user. We can update  $E_{max}^k$  according to:

$$E_{max}^k = r_1 e^{-r_2 \sum_{i=1}^n deg_i} + (1 - r_1) e^{\sum_{i=1}^n deg_i} \quad (30)$$

where,  $r_1$  and  $r_2$  are two coefficients and  $deg_i$  represents the degradation rate. We refer the readers to [21] and [22] for specific procedures of degradation rate calculation and other details.

The OM optimization model described here is also a non-convex MIQCQP like the base dispatch OM model. Both OM models have the same number of constraints. However, this extended OM model has two additional types of decision variables and two new quadratic terms in the objective function for each ST ground arc and vehicle.

### C. Model-RS: eVTOL Fleet Dispatch Model for Providing Only Frequency Regulation Services

An OM model may also be formulated to optimally dispatch the eVTOL fleet for the sole purpose of providing frequency regulation services. In such a case, the eVTOLs would remain on the ground at different charging/discharging stations of the vertiports throughout the period of operation for two reasons. Firstly, no passengers would be transported by the vehicles. Secondly, because we are assuming that the price of electricity is same at all vertiports at any given time instance, there is no incentive to reposition the vehicles during the operational period.

This model, referred to as model-RS, can be derived by removing all decision variables, terms and equations related to providing UAM travel service from model-TRS. As no passenger would be served and no flights would be flown, the objective function would now no longer have the  $R_T$  and  $C_O$  components, as shown in Eq. 31. For the same reason, the decision variables  $p_{ij}$ ,  $w_{ij}$ , and  $x_{ij}^k$  corresponding to ST flight arcs  $(i, j)$  would also not be present in this model; moreover, equations related to ST arc demand and passenger capacity, as given in Eqs. (5)-(8), are also no longer needed.

$$\max z = R_R - C_C \quad (31)$$

The vertiport assignment constraint and vehicle flow conservation constraints, given in Eqs. (9)-(11), would still be applicable. However, the vehicle flow conservation constraints would now no longer need to take into account the incoming and outgoing ST flight arcs, as expressed in Eqs. (32) and (33). As the vehicles will continue to stay in the same vertiport after the initial assignment during the operational period, only the initial vertiport capacity constraint, given in Eq. 12, is needed. All the energy constraints of model-TRS except the flight arc energy constraint, given in Eq. (17), would also be present in model-RS.

$$x_i^k = x_{ij}^k, \quad \forall i \in N' : i = (\hat{i}, 0), j = (\hat{i}, s), (i, j) \in A', \forall k \in K \quad (32)$$

$$x_{ih}^k = x_{hj}^k, \quad (33)$$

$$\forall h \in N' : h = (\hat{h}, r), 1 \leq r \leq |T| - 1, i = (\hat{h}, s), j = (\hat{h}, t), (i, h) \in A', (h, j) \in A', \forall k \in K$$

Like the previous two models, model-RS is also a non-convex MIQCQP. However, the number of decision variables and constraints is fewer than model-TS and model-TRS. So, solving model-RS is computationally less expensive.

## VI. Simulation Environment

In this section, we describe the simulator used for modeling the eVTOL fleet operations in a UAM network with time-varying passenger demand and electricity market conditions. The simulator gives the required problem inputs to the OM model, which then uses it to determine the optimal dispatching and pricing solution. This solution of the current time step is fed back to the simulator, which uses it to update the position of the vehicles and the state of their batteries, and current passenger demand in the various routes within the network. This process takes place at the beginning of every time step and it continues until the end of the simulation (or operational) period. The profit earned and the values of the decision variables of the OM model can be obtained at the end of simulation. All the OM models are in turn used with the simulator to record and compare their performances.

The simulator was built in MATLAB. It consists of four parts: 1) vertiport model, 2) vehicle model, 3) passenger demand model, and 4) electricity market model. Each of these models is described in the following subsections.

### A. UAM Network Model

Three fully connected vertiports that are equidistant from each other forms the UAM network. So, there are 6 distinct routes in total. In each of these routes, the trip time is considered to be less than or equal to  $T^I$  (30 mins) and the flight distance is 24.85 miles, which is within the range of most eVTOLs currently being developed. All vertiports are assumed to have a capacity of 6 eVTOLs. In other words, there are 6 takeoff and landing areas and 6 high voltage charging/discharging stations in each vertiport. So,  $u_1 = u_2 = u_3 = 6$ . At each charging/discharging station, a eVTOL can charge its battery to replenish the depleted energy and charge/discharge to provide frequency regulation services during its ground time with an assumed  $P_{max}$  value of 150 kW.

In the corresponding ST UAM network, the 6 ST nodes within each time step is fully connected. So, there are 6 ST flight arcs and 3 ST ground arcs in each time step. This means that an eVTOL  $k$  at a vertiport  $\hat{i}$  at time  $r$  can either be dispatched on a ground arc to stay at the same vertiport in the current time step or be dispatched on a flight arc to fly to

any of the other two vertiports such that it reaches its destination by the end of the current time step. As  $T^I = 30$  min, the number of time steps per day is 48.

## B. Vehicle Model

The vehicle model defines the dynamical model and battery model of the eVTOL vehicles in the simulation. It is based on the fully autonomous and electric CityAirbus vehicle being developed by Airbus for use as an air taxi [26], as shown in Fig. 3. Its first unmanned flight test was conducted in May 2019. Following the CityAirbus model's technical specifications, the vehicle passenger capacity  $C$  is set to 4, cruise speed to 74.56 mph and battery capacity  $E_{max}^k$  to 110 kWh (the combined battery capacity of its four batteries) in our vehicle model. Given the cruise speed and route flight distance, the duration of each flight is 20 mins. The eVTOL fleet of the UAM carrier is considered to be made up of 9 eVTOLs.



**Fig. 3** The CityAirbus eVTOL aircraft

The simulator also contains a battery model for each eVTOL to keep track of its current energy level and battery capacity. The energy level of the eVTOLs change with time due to energy expenditure or consumption during the flight and charging/discharging operations, while the battery capacity of eVTOLs change with time due to battery degradation. The battery capacities are assumed to represent only the useable fraction of energy, i.e., it does not include any reserves for protecting the battery function. The degradation of an eVTOL's battery was modeled using Eq. 30. In practice, when the degradation level of the battery drops below a certain threshold, a replacement cost for the battery will be incurred. The self discharge amount of the batteries was considered to be 1.65% per month. So, as  $T^I = 30$  min, the self discharge rate of the batteries  $\gamma$  in each time step is equal to  $1.65/(100 \cdot 30 \cdot 24 \cdot 2) = 1.15 \times 10^{-5}$ .

The eVTOL operating cost per mile was estimated to approach \$0.64 in the near-term based on cost factors such as vehicle maintenance cost, infrastructure costs, piloting costs, recharging costs, capital expenses and other operating expenses in [1]. In this work, the definition of flight operating cost includes only the vehicle maintenance cost and autonomous piloting technology costs. The flight operating cost per mile was considered to be \$0.6. So, given route distances of 24.85 miles, the flight operating cost ( $c_{ij}$ ) at all ST flight arcs ( $i, j$ ) is \$14.91.

## C. Passenger Demand Model

The passenger demand model is used to generate stochastic passenger flight requests at each ST flight arc. Potential passenger demand for UAM services has been estimated in past studies using data sources such as helicopter charter services, census data, and consumer wealth data [27, 28]. For this research, the mean potential passenger demand in the various ST flight arcs of each day was estimated based on the hourly distribution given for each trip purpose (commute, family/personal, school/church, recreational and other) for the annual trips per start time by the Federal Highway Administration [29]. A stacked bar chart showing the variation of the mean potential demand in the various routes at different times of a day is given in Fig. 4. During simulation, the actual or real-time potential passenger demand at each ST flight arc ( $i, j$ ) ( $q_{ij}$ ) was generated by sampling from a normal distribution with a mean set equal to the mean potential passenger demand of the ST flight arc ( $i, j$ ) and a standard deviation set to 2. Before the start of any given time step, the UAM carrier knows the actual potential passenger demand in the ST arcs associated with the current time step and the forecasted potential passenger demand in the ST arcs associated with the future time steps of the planning horizon. In practice, the UAM carrier may forecast the demand by using various qualitative and/or quantitative demand forecasting methods. The UAM carrier's forecasted potential demand of the ST arcs is considered

to be equal to the mean potential demand of the ST arcs in the simulator. These ST arc demands are provided to the OM model before it is solved at the start of each time step.

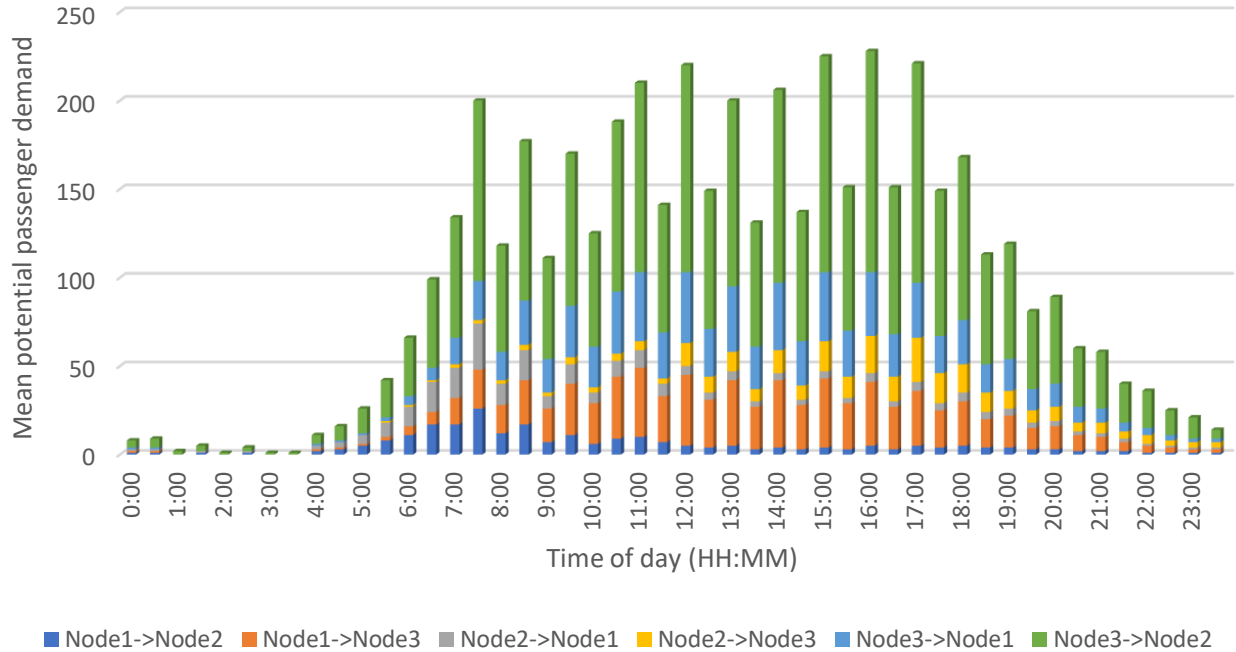


**Fig. 4** Stacked bar chart of mean potential passenger demand in the various routes at different times of a day

#### D. Electricity Market Model

The electricity market model provides the OM model with electricity market prices and frequency regulation signals ( $LMP_r$ ,  $B_r^U$ ,  $B_r^D$ ,  $P_r^U$  and  $P_r^D$ ) values of the current time step and their forecasted values for the future time steps in the planning horizon. Towards this end, it uses historic electricity market data collected from PJM [30], which includes the hourly electricity prices ( $LMP_r$ ), hourly revenues of providing regulation services ( $B_r^U$  and  $B_r^D$ ), and regulation signals ( $P_r^U$  and  $P_r^D$ ). Given the frequency regulation signals are updated every 2 seconds, the electricity market model uses the average of regulation up and down signals over a 30 minutes interval in this study.

Just like the passenger demand information, before the start of any given time step, the UAM carrier knows the exact values of electricity market prices and signals in the current time step and their forecasted values for the future time steps of the planning horizon. The exact value for each market variable at each time step is obtained from the data used by the electricity market model. In practice, the UAM carrier can adopt machine learning techniques, e.g., deep neural networks, to forecast the real-time electricity market prices for each future time step of the planning horizon [31]. Deep neural networks take certain related features and output the predictions. In this case, the related input features include weather forecast, electric load forecast, renewable generation forecast, fuel price, historic electricity prices, etc. The output is the real time electricity price forecast. In the electricity market model, the forecasted power grid parameter values at a given time step are computed by an averaging process. For each parameter, there are 48 daily values for the 48 time steps in a day in the data. These chronologically ordered values are divided into four equal groups each of which span 6 hours. Group 1 values correspond to the time steps within 00:00-06:00, group 2 values correspond to the time steps within 06:00-12:00, and so on. The forecasted value of the parameters at any time step belonging to one of these groups is assumed to be equal to the average of the corresponding parameter values of that group. The exact current time step values and forecasted parameter values are provided to the OM model before it is solved at the start of each time step.

**Table 1 Financial performance results of model-TS, model-RS and model-TRS**

	Model-TS	Model-RS	Model-TRS
$\mu_z$ (\$)	22159	1524.3	22922
$\sigma_z$ (\$)	534.15	641.62	701.54
95% CI $_z$ (\$)	$\pm 200$	$\pm 239.6$	$\pm 262$
$\mu_{R_T}$ (%)	100	0	96.41
$\sigma_{R_T}$ (%)	0	0	1.17
95% CI $_{R_T}$ (%)	$\pm 0$	$\pm 0$	$\pm 0.44$
$\mu_{R_R}$ (%)	0	100	3.59
$\sigma_{R_R}$ (%)	0	0	1.17
95% CI $_{R_R}$ (%)	$\pm 0$	$\pm 0$	$\pm 0.43$

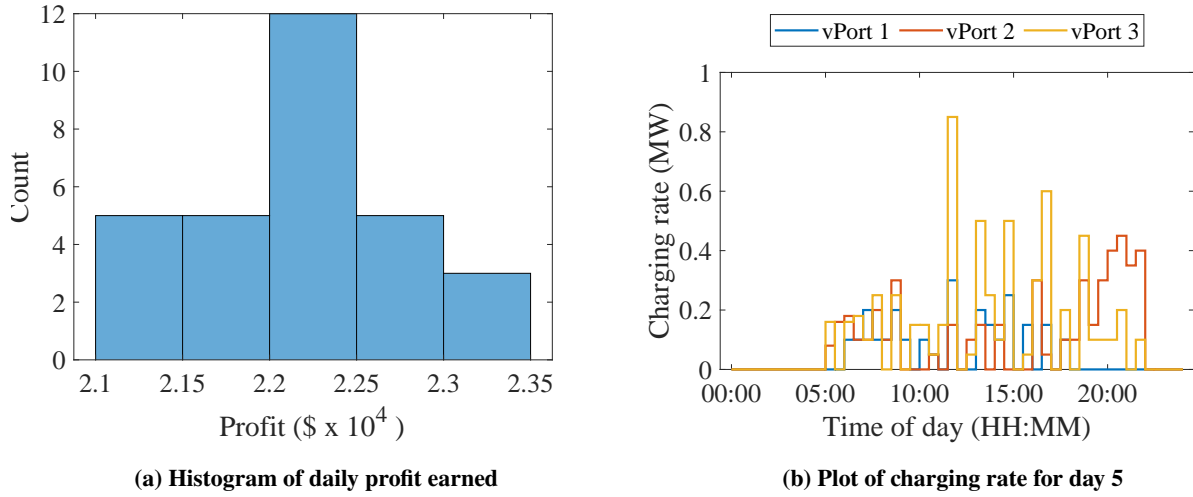


**Fig. 5 Financial performance and energy expenditure graphs of model-TS**

## VII. Results

The performance of all three OM models were evaluated separately in the simulator and compared with each other to determine the best service(s) to provide by the UAM carrier. For each of the models, the planning horizon was specified to be 2 hours (4 time steps) and the planning frequency to be 1 (the OM model was re-solved once after each time step). Within the duration of the planning horizon, there are 36 ST arcs, of which 12 are ground arcs and 24 are flight arcs. The duration of total operation was set to 30 days in the simulator. The energy market data of July 1st till July 30th of the year 2019 was used in the simulation, whereas the demand data was generated for the 30 days using the process described in the preceding section. As the simulation was carried out for only 30 days, the battery degradation effect were negligible and thus ignored. Typically, the battery degradation effect becomes significant after one year of battery usage. Our framework is capable of capturing this effect through Eq. 30.

The models were solved using the Gurobi Optimizer. For each day of the simulation, the operating profit ( $z$ ), revenue from travel service ( $R_T$ ), revenue from regulation service ( $R_R$ ) and decision variable values associated with each ST arc and vehicle were recorded. The key financial performance indicators of the models are summarized in Table 1, where  $\mu$ ,  $\sigma$  and 95% CI denote the mean, standard deviation and 95% confidence interval respectively, and the subscripts  $z$ ,  $R_T$ , and  $R_R$  denote the daily profit, revenue attributed to travel services, and revenue attributed to regulation services respectively like before. Note that  $R_T$  and  $R_R$  are now expressed as percentages of the daily total revenue.

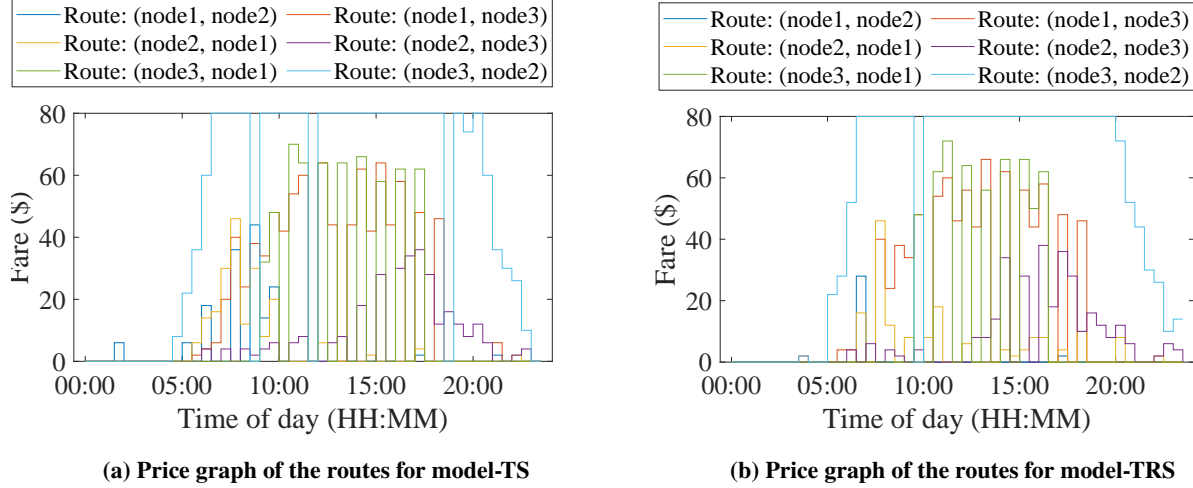


**Fig. 6 Price graph of the routes in the UAM network**

### A. Model-TS

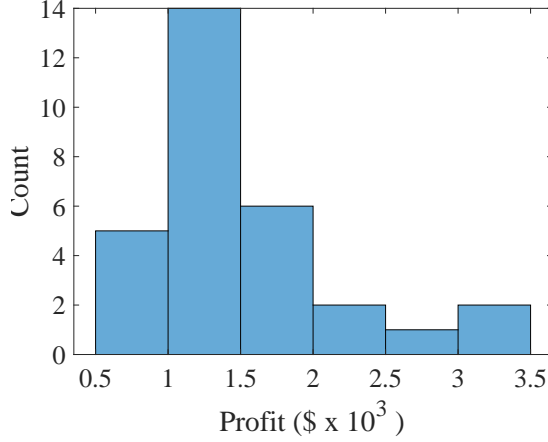
As shown in Table 1, model-TS was able to earn a daily profit of \$22,159 on average with a standard deviation of \$534.15 and a 95% CI of  $\pm$ \$200. As the only source of revenue for model-TS is the travel service provided to passengers,  $\mu_{RT}$  is 100% and  $\mu_{RR}$  is 0%. The histogram of the daily profit earned is illustrated in Fig. 5a, which shows that daily profit earned lies between \$22500 and \$22000 on 12 out of the 30 days, and is spread almost uniformly across the other bins of the histogram. Fig. 6a shows how the fare charged at different routes is varied with time by model-TS. Setting the fares optimally at each time step is key to maximizing the total transportation revenue generated. As demand is very low during the first 4 hours of the day, the fares set in all the routes are low as well. After that initial period, demands in the routes start increasing and, so, model-TS optimally sets increasingly higher fares in the routes based on the demand and available seat capacity. During the last part of the day, the drop in demand causes the model-TS to set lower fares. As the routes (node3, node1) and (node3, node2) have higher demands than the other routes, the fares charged in those routes are also higher.

The plot of charging rate given in Fig. 5b shows how the total charging rate amount varies throughout day 5 of the simulation at all vertiports. The total charging rate at any vertiport at any time step is the sum of the individual vehicle charging rates at that vertiport at that time step. As model-TS does not engage the eVTOLs in providing frequency regulation services, the eVTOLs do not discharge and, hence, the charging rate never goes below zero throughout the day. Among the three vertiports, the charging rate of the vehicles at vertiport 3 is higher than those of the other vertiports at most time steps. This occurs because the model dispatches most of the eVTOLs to vertiport 3 repeatedly throughout the day to serve the high passenger demand in the (node3, node1) and (node3, node2) routes throughout the day as shown in Fig. 4.

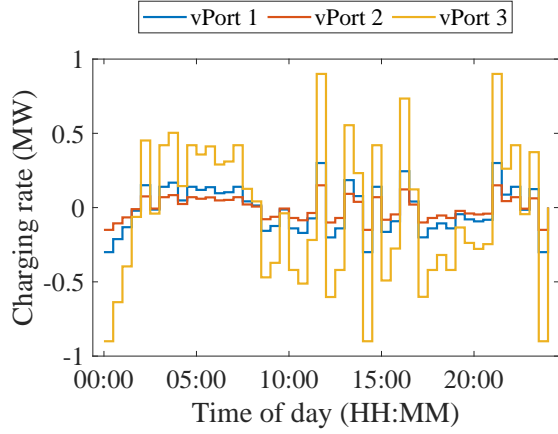
### B. Model-RS

By providing only frequency regulation services to the power grid ( $\mu_{RT} = 0\%$  and  $\mu_{RR}$  is 100%), model-RS was able to earn a mean daily profit of \$1524.3, which is an order of magnitude lower than that of model-TS and model-TRS. This implies that the transportation of passengers is the primary source of revenue for the UAM carrier in this simulation, given the passenger demand in the ST flight arcs (the different routes at different times of the operational period). Unless the passenger demand is extremely low, model-RS cannot compete with model-TS and model-TRS in terms of profit. However, the daily profit earned by model-RS suggests that providing frequency regulation services can be a secondary source of revenue for the UAM carriers, especially during periods of low demand. The values of  $\sigma_z$  and 95% CI<sub>z</sub> of model-RS is similar to that of the other two models. Fig. 7a shows the histogram of the daily profit of model-RS, which, unlike the symmetric histograms of the other models, is skewed right.

The charging rate plot for day 5 of model-RS is given in Fig. 7b. Note that the total charging rate amount is positive for almost half of the day and negative for the rest of the day, indicating that the eVTOLs are solely providing frequency regulation services by charging and discharging with time based on the regulation signals given by the electricity market

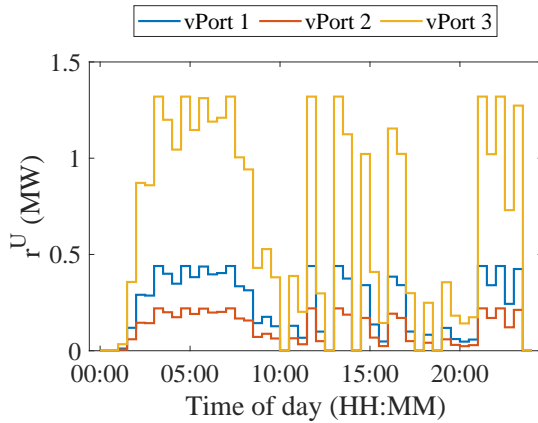


(a) Histogram of daily profit

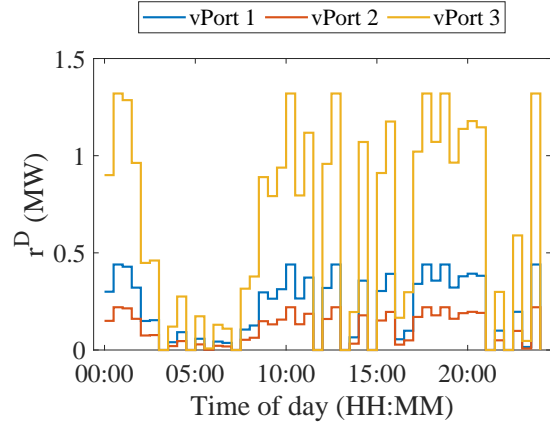


(b) Plot of charging rate for day 5

**Fig. 7 Financial performance and energy expenditure graphs of model-RS**



(a) Plot of capacity provided to regulation up service for day 5



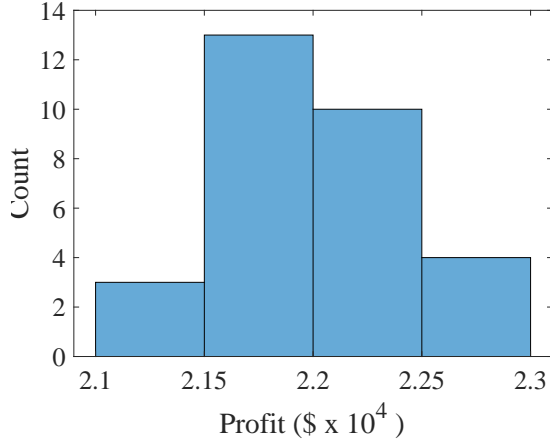
(b) Plot of capacity provided to regulation down service for day 5

**Fig. 8 Provided capacities for frequency regulation services by model-RS for day 5**

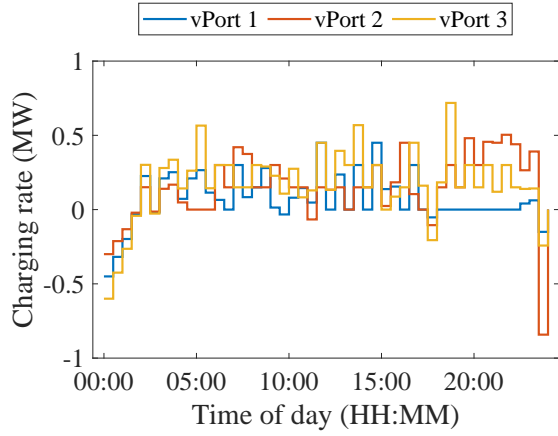
model of the simulator. The plots of provided capacities at the different vertiports for regulation up and down services are given in Figs. 8a and 8b respectively, where  $r^U$  and  $r^D$  denote the total provided capacity for regulation up and down services at a given vertiport respectively. Once again, the energy exchange activity with the power grid appears to be highest at vertiport 3 as the model has assigned most of the vehicles there. Note that the vertiport assignment of the vehicles does not affect the daily profit earned by model-RS as the power grid parameters are assumed to be the same at all vertiports at any given time step.

### C. Model-TRS

Among all three models, model-TRS can be observed to earn the highest mean daily profit in Table 1. Its  $\mu_z$  exceeds that of model-TS and model-RS by \$763 and \$21397.7 respectively. Relative to model-TS, the mean daily incremental profit of \$763 leads to an approximate mean yearly increment of \$278495. This higher  $\mu_z$  is a result of generating revenues from both the UAM travel market and energy market simultaneously using the same fleet of eVTOLs. Out of the total daily revenues generated, 96.41% comes from providing travel services and the rest 3.59% from frequency regulation services on average. Fig. 9a shows the histogram of the daily profit of model-TRS. Fig. 6b shows how the fare charged at different routes is varied with time by model-TRS. It is similar to the price graph of model-TS as model-TRS also optimally sets the route fares based on the demand and available seat capacity in the routes.

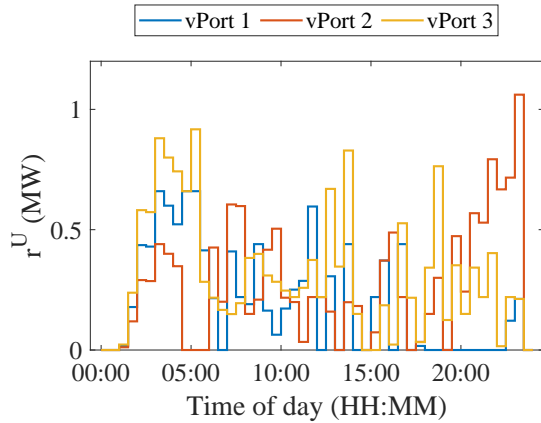


(a) Histogram of daily profit

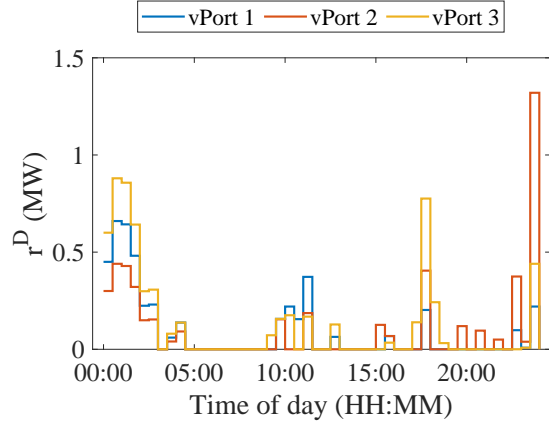


(b) Plot of charging rate for day 5

**Fig. 9 Financial performance and energy expenditure graphs of model-TRS**



(a) Plot of capacity provided to regulation up service for day 5



(b) Plot of capacity provided to regulation down service for day 5

**Fig. 10 Provided capacities for frequency regulation services by model-TRS for day 5**

The charging rate plot for day 5 of model-TRS is given in Fig. 9b. At all vertiports, the vehicles can be seen discharging mostly during the first and last few hours of the day. For the rest of the time, the vehicles are mostly charging for either restoring battery energy for future flights or to provide regulation services. The plots of provided capacities at the different vertiports for regulation up and down services are given in Figs. 10a and 10b respectively. Compared to model-RS, the values of  $r^U$  and  $r^D$  and the areas under the curves for model-TRS are lower. This indicates that model-TRS provides less frequency regulation service than model-RS. During the first and last part of the day, when the route demands are low,  $r^U$  and  $r^D$  are higher than at other times of the day. This indicates that the model focuses more on providing frequency regulation services than transportation services during periods of low demand, allowing it to generate additional revenue and thus earn higher a total profit relative to model-TS.

## VIII. Conclusion

The problem of eVTOL fleet dispatching from the perspective of an UAM carrier is considered in this paper. As the nature of operations involved in UAM is different than that in traditional aviation and ground transportation, new dispatch models are needed to take into account the unique aspects of this operation. In addition to generating revenue from transporting passengers, we envision that UAM carriers can generate additional revenue from providing frequency

regulation services to the power grid using the batteries in the eVTOL fleet. To address the problem of eVTOL fleet dispatching and analyze the financial impact of this new revenue source, we have formulated three different eVTOL fleet dispatch models in this study: 1) model-TS for providing only travel services; 2) model-RS for providing only frequency regulation services; and 3) model-TRS for providing both travel and frequency regulation services simultaneously. Model-TS and model-TRS can also determine the optimal fare to charge passengers for each flight. The performance of the models were evaluated using a simulator. The eVTOL vehicle fleet operations was subjected to two sources of uncertainties: the pricing/incentive stochasticity from the dynamic electricity market, and the passenger demand uncertainty arising from the stochastic trip requests. Model-TS is an extension of our previous OM model [24]. Among all three models, model-TRS was observed to earn the highest mean daily profit in our simulation. More specifically, the mean daily profit of model-TRS exceeded that of model-TS and model-RS by \$763 and \$21397.7 respectively. Model-TRS achieved this by optimally trading off between maximizing revenue from the UAM travel market and electricity market and minimizing flight operating and charging costs. During periods of low demand, model-TRS was found to focus more on providing frequency regulation services than transportation services, enabling it to generate surplus revenue and thus earn higher a total profit relative to model-TS. Both model-TS and model-TRS were found to optimally set the route fares based on the demand and available seat capacity in the routes.

There are several promising extensions of this work that form exciting topics for future research. First, additional sources of revenue from trading electricity in the day-ahead and real-time energy market, and providing energy reserve, cargo transportation and eVTOL rental services can be incorporated in model-TRS to examine their impact on profit earnings and fleet dispatching. Second, uncertainties in flight times can be considered in the eVTOL fleet dispatching problem to make the models more practical. Also, the dependence of flight energy expenditure of the eVTOLs on the weight of its payload can be considered in the problem to improve the models' tracking of eVTOL energy levels. Third, time can be treated as either continuous or the time steps can be reduced in duration to a few minutes to enable the models to make dispatching decisions more frequently in near real-time.

## References

- [1] Holden, J., and Goel, N., "Fast-Forwarding to a Future of On-Demand Urban Air Transportation," *San Francisco, CA*, 2016.
- [2] Volocopter, "Reinventing Urban Mobility," <http://www.volocopter.com/en>, 2019. (Accessed: 2019-11-05).
- [3] Aurora, "eVTOL," <http://www.aurora.aero/evtol>, 2019. (Accessed: 2019-11-05).
- [4] Joby Aviation S2, "S2," <http://www.jobyaviation.com/S2>, 2019. (Accessed: 2019-11-05).
- [5] Airbus, "Vahana," <http://www.airbus-sv.com/projects/1>, 2019. (Accessed: 2019-11-05).
- [6] Zee Aero, "Cora," <http://www.cora.aero>, 2019. (Accessed: 2019-11-05).
- [7] Airbus, "Rethinking Urban Air Mobility," <http://www.airbus.com/newsroom/topics-in-focus/urban-air-mobility.html>, 2019. (Accessed: 2019-11-05).
- [8] Mueller, E. R., Kopardekar, P. H., and Goodrich, K. H., "Enabling Airspace Integration for High-Density On-Demand Mobility Operations," *17th AIAA Aviation Technology, Integration, and Operations Conference*, 2017, p. 3086.
- [9] Vascik, P. D., Hansman, R. J., and Dunn, N. S., "Analysis of urban air mobility operational constraints," *Journal of Air Transportation*, Vol. 26, No. 4, 2018, pp. 133–146.
- [10] Schmid, V., "Solving the dynamic ambulance relocation and dispatching problem using approximate dynamic programming," *European journal of operational research*, Vol. 219, No. 3, 2012, pp. 611–621.
- [11] Moon, M., "Dubai tests a passenger drone for its flying taxi service," <http://www.engadget.com/2017/09/26/dubai-volocopter-passenger-drone-test>, 2017. (accessed November 20, 2018).
- [12] Thipphavong, D. P., Apaza, R., Barmore, B., Battiste, V., Burian, B., Dao, Q., Feary, M., Go, S., Goodrich, K. H., Homola, J., et al., "Urban air mobility airspace integration concepts and considerations," *2018 Aviation Technology, Integration, and Operations Conference*, 2018, p. 3676.
- [13] Bosson, C., and Lauderdale, T. A., "Simulation Evaluations of an Autonomous Urban Air Mobility Network Management and Separation Service," *2018 Aviation Technology, Integration, and Operations Conference*, 2018, p. 3365. doi:10.2514/6.2018-3365.

- [14] Wang, W., and Yu, N., “LMP decomposition with three-phase DCOPF for distribution system,” *2016 IEEE Innovative Smart Grid Technologies - Asia (ISGT-Asia)*, 2016, pp. 1–8.
- [15] Liu, Y., Yu, N., Wang, W., Guan, X., Xu, Z., Dong, B., and Liu, T., “Coordinating the operations of smart buildings in smart grids,” *Applied Energy*, Vol. 228, 2018, pp. 2510–2525.
- [16] “Market for Electricity,” <https://learn.pjm.com/electricity-basics/market-for-electricity.aspx>, 2019.
- [17] Yu, N.-P., Liu, C.-C., and Price, J., “Evaluation of market rules using a multi-agent system method,” *IEEE Transactions on Power Systems*, Vol. 25, No. 1, 2009, pp. 470–479.
- [18] Wang, W., and Yu, N., “Chordal conversion based convex iteration algorithm for three-phase optimal power flow problems,” *IEEE Transactions on Power Systems*, Vol. 33, No. 2, 2017, pp. 1603–1613.
- [19] Wang, W., Abdolrashidi, A., Yu, N., and Wong, D., “Frequency regulation service provision in data center with computational flexibility,” *Applied Energy*, Vol. 251, 2019, p. 113304.
- [20] “PJM manual 11: Energy & ancillary services market operations,” Tech. rep., PJM, 2019.
- [21] Zhang, Z., Shi, J., Gao, Y., and Yu, N., “Degradation-aware Valuation and Sizing of Behind-the-Meter Battery Energy Storage Systems for Commercial Customers,” *2019 IEEE PES GTD Grand International Conference and Exposition Asia (GTD Asia)*, IEEE, 2019, pp. 895–900.
- [22] Foggo, B., and Yu, N., “Improved battery storage valuation through degradation reduction,” *IEEE Transactions on Smart Grid*, Vol. 9, No. 6, 2017, pp. 5721–5732.
- [23] Yu, N., and Foggo, B., “Stochastic valuation of energy storage in wholesale power markets,” *Energy Economics*, Vol. 64, 2017, pp. 177–185.
- [24] Shihab, S. A. M., Wei, P., Ramirez, D. S. J., Mesa-Arango, R., and Bloebaum, C., “By Schedule or On Demand?-A Hybrid Operation Concept for Urban Air Mobility,” *AIAA Aviation 2019 Forum*, 2019, p. 3522.
- [25] Kannan, H., Shihab, S., Zellner, M., Salimi, E., Abbas, A., and Bloebaum, C. L., “Preference modeling for government-owned large-scale complex engineered systems: a satellite case study,” *Disciplinary Convergence in Systems Engineering Research*, Springer, 2018, pp. 513–529.
- [26] Airbus, “CityAirbus,” <https://www.airbus.com/innovation/urban-air-mobility/vehicle-demonstrators/cityairbus.html>, 2019. (Accessed: 2020-05-10).
- [27] Vascik, P. D., and Hansman, R. J., “Constraint identification in on-demand mobility for aviation through an exploratory case study of los angeles,” *17th AIAA Aviation Technology, Integration, and Operations Conference*, 2017, p. 3083.
- [28] Alonso, J. J., Arneson, H. M., Melton, J. E., Vegh, M., Walker, C., and Young, L. A., “System-of-Systems Considerations in the Notional Development of a Metropolitan Aerial Transportation System.[Implications as to the Identification of Enabling Technologies and Reference Designs for Extreme Short Haul VTOL Vehicles With Electric Propulsion],” 2017.
- [29] US Department of Transportation, Federal Highway Administration, “Our Nation’s Highways: 2010,” [https://www.fhwa.dot.gov/policyinformation/pubs/hf/pl10023/fig4\\_6.cfm](https://www.fhwa.dot.gov/policyinformation/pubs/hf/pl10023/fig4_6.cfm), 2019. (Accessed: 2019-05-13).
- [30] “Data Miner 2,” <https://www.pjm.com/markets-and-operations/etools/data-miner-2.aspx>, 2020.
- [31] Wang, W., and Yu, N., “A Machine Learning Framework for Algorithmic Trading with Virtual Bids in Electricity Markets,” *2019 IEEE Power & Energy Society General Meeting (PESGM)*, IEEE, 2019, pp. 1–5.